Pulsed-Laser Polymerization in Compartmentalized Liquids. 1. Polymerization in Vesicles

Martin Jung, Ilse van Casteren, Michael J. Monteiro, Alex M. van Herk,* and Anton L. German

Laboratory of Polymer Chemistry and Coatings Technology, Eindhoven University of Technology, P.O. Box 513, 5600 MB Eindhoven, The Netherlands

Received November 15, 1999; Revised Manuscript Received February 17, 2000

ABSTRACT: Polymerization in vesicles is a novel type of polymerization in heterogeneous media, leading to parachute-like vesicle−polymer hybrid morphologies. To explore the kinetics of vesicle polymerizations and to learn more about the actual locus of polymerization we applied the pulsed-laser polymerization (PLP) technique to the polymerization of styrene in small and large unilamellar dioctadecyldimethylammonium bromide (DODAB) vesicles. The analysis of the molecular weight distribution (MWD) allows primarily the determination of the monomer concentration at the site of polymerization if the propagation rate coefficient, k_p, of the applied monomer is known. Relatively high monomer concentrations (between 2.6 and 4.5 mol/L) were found at the locus of polymerization at low conversions. PLP experiments as a function of overall monomer concentration, temperature, and vesicle size gave insight into the monomer partitioning between vesicle and polymerization site. With respect to the mechanism of polymerization in vesicles, the observations seem to indicate that polymerization occurs in a small polymer nucleus where high monomer concentrations are encountered.

Introduction

Polymerization *in* Vesicles. The self-assembly structures of amphiphiles in water provide ideal reaction media for heterogeneous polymerizations.[1−3] The polymerization *kinetics* and the polymer *morphology* depend largely on the initial amphiphile aggregate structure. In most cases, globular micelles are employed, e.g. for the whole family of emulsion polymerization reactions (microemulsion, miniemulsion, and emulsion polymerization), leading to spherical latices.[4] To open the way to new morphologies, *vesicles* have recently attracted considerable interest as a reaction medium for the free-radical polymerization of standard monomers.[5−11] The concept was to employ the *closed hollow bilayer surfactant structure* of a vesicle as a *template* for the polymerization of monomers that are solubilized within the vesicle bilayer. By polymerization of the solubilized monomer, it was intended to transform the amphiphile aggregate structure into a hollow polymeric architecture. Although this concept seems simple, there is a strong interplay between the kinetics of polymerization and the changing thermodynamics of the system bilayer/monomer/polymer. Therefore, it is not unexpected to find that the resulting vesicle−polymer *morphology* is currently a matter of debate. Several research groups have claimed that polymerization in vesicles was indeed a feasible route to synthesize hollow polymer particles.[5−10] In contrast, our own investigations on the polymerization of styrene in dioctadecyldimethylammonium bromide (DODAB) vesicles proved that the polymerization in these vesicles leads to phase separation between amphiphile and polymer, resulting in the so-called parachute morphology[11] (so-called because of the appearance when visualized by cryo-TEM; see Figure 1). We further showed that the *monomer* is uniformly distributed over the bilayer at the beginning of the reaction,[12] whereas the *polymer* is entirely phase separated from the bilayer after the polymerization.[13] Nonetheless, the polymer stays attached to the bilayer as a polystyrene bead. A detailed on-line SANS study[14] revealed that the phase separation between polymer and surfactant matrix takes place within the very early stages of the polymerization process (schematically illustrated in Figure 2). Virtually the first polymer chains create an ellipsoidal polymer nucleus (step 1) which gradually grows in size (step 2) and attains a more spherical geometry with progressing conversion (step 3). The final size of the attached polymer bead is

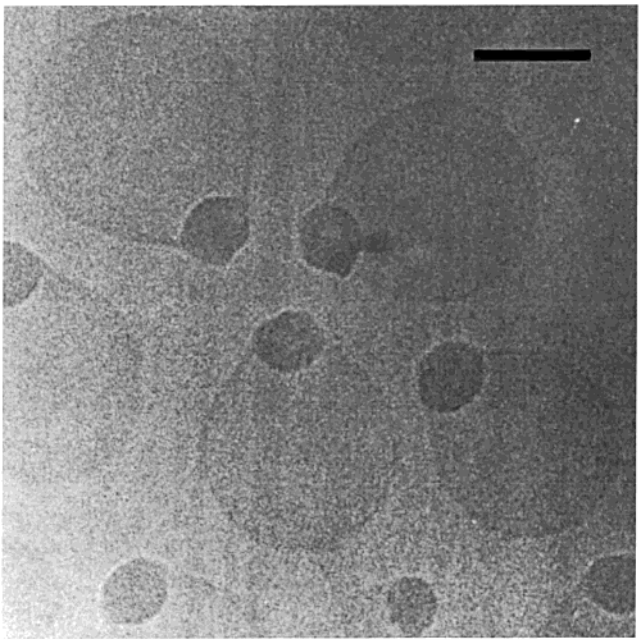

Figure 1. Cryo−TEM micrograph after polymerization of styrene in extruded DODAB vesicles. Parachute-like polymer−vesicle morphologies are observed. Scale bar corresponds to 100 nm.

* To whom correspondence should be sent. E-mail: A.M.v.Herk@TUE.NL.

10.1021/ma9919211 CCC: $19.00
Published on Web 04/21/2000

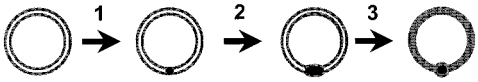

Figure 2. Schematic representation of the morphological evolution during polymerization in vesicles. The dark gray layers represent the bilayer halves while the light gray part symbolizes the solubilized monomer, and the black parts mark the polymer.

predetermined by the amount of solubilized monomer in the parental vesicle, i.e., the bead size depends on the diameter of the vesicle *and* its monomer load. The polymerization of styrene in *s*mall *u*nilamellar *v*esicles (SUVs, diameter 40 nm) yields polymer beads of ∼25 nm diameter while *l*arge *u*nilamellar *v*esicles (LUVs, diameter 160 nm) produce larger beads of ∼58 nm diameter.[13]

Aim of This Study. Despite the detailed morphological knowledge on the final vesicle−polymer architecture and its evolution in time, it stays unanswered where the polymerization actually proceeds. Does chain propagation occur in the bilayer or does it take place in the phase-separated polymer locus? An answer to this question could be given if we obtained more characteristics of the polymerization locus itself. The monomer concentration at the locus of polymerization is one highly interesting parameter that plays a significant role in the inherent polymerization kinetics of compartmentalized systems.[15] This *local* monomer concentration bears unique information on the environment that a growing polymer chain actually experiences, or in other words, it provides insight in the spatial distribution of monomer and so reflects the morphology of the *polymerization locus*.

Here, we apply the *p*ulsed-*l*aser *p*olymerization (PLP) technique to the polymerization of styrene in vesicular structures in order to determine experimentally the *concentration of the monomer at the site of reaction* throughout the polymerization in vesicles and thus explore the nature of the *locus* of polymerization in vesicles. These data should help to augment our understanding of kinetic features of polymerization in vesicles. Two types of DODAB vesicles will be compared: small unilamellar vesicles, prepared by sonication, and large unilamellar vesicles prepared by extrusion.[31]

Along the way, we report some peculiar observations for PLP experiments in compartmentalized systems and discuss typical experimental problems.

The PLP Method. One method used to determine the concentration of monomer at the *locus of polymerization* by *kinetic* means is the pulsed-laser polymerization/SEC method.[16−23] This method is designed as a combination of a pulsed-laser polymerization and the determination of the obtained molecular weight distribution (MWD) by size exclusion chromatography (SEC). A pulsed-laser polymerization comprises the generation of radicals out of a photoinitiator, activated by a laser pulse. During the dark time, i.e., the time between subsequent pulses, a significant amount of chains keep on propagating while termination occurs preferably just after a laser pulse when the radical concentration is increased. If this procedure is repeated with a constant laser frequency, the resulting *molecular weight distribution* exhibits one or more peaks that correspond to polymer chains that have grown an integer multiple, i, of the time between successive pulses, t_0. The chain length of these chains can be described by

$$L_{0,i} = ik_p[\mathrm{M}]t_0 \qquad (1)$$

where $L_{0,i}$ is the length of the polymer formed by linear growth in the time between two laser pulses, it_0, k_p the propagation rate coefficient, and [M] the monomer concentration at the site of polymerization. The chain length of the polymer, $L_{0,i}$, can be experimentally obtained by SEC. The low molecular weight inflection point of the molecular weight distribution on logarithmic scale, $w(\log M)$, is taken as the best measure of $L_{0,i}$.[23] In principle, the PLP−SEC technique allows one to measure the propagation frequency, k_p[M], which can be interpreted in two ways. If the monomer concentration is exactly known, as in bulk or solution systems, then the propagation rate coefficients, k_p, can be determined.[16] Alternatively, the concentration at the site of reaction, [M], can be found by this method using the previously measured value of k_p. The latter application has proved success for the study of heterogeneous systems such as microemulsions[24−26] and latices.[27−30] An application to the polymerization of styrene in vesicles should equally be viable. For our calculations we use the IUPAC value of k_p for styrene,[17] given by

$$k_p = 10^{7.63} \exp\left(\frac{-32.51 \times 10^3}{RT}\right) \mathrm{L/mol{\cdot}s} \qquad (2)$$

where R [J/mol·K] represents the gas constant and T [K] the absolute temperature.

Experimental Section

Materials. Dioctadecyldimethylammonium bromide (DODAB, Fluka, >98%) was purified by repeated crystallization from ethyl acetate. Styrene (Merck, >99%) was distilled under reduced pressure and stored at −18 °C. The oil-soluble photoinitiator 2,2-dimethoxy-2-phenylacetophenone (DMPA, Aldrich, 98%) was used as received. Super-Q water (Millipore) was used to prepare the vesicles.

Vesicle Preparation. Vesicles were either prepared by sonication or by the extrusion process.[31] Prior to preparation, a 1×10^{-2} mol/L DODAB in water dispersion was allowed to hydrate at 60 °C for 2 days.[12] Small unilamellar vesicles were obtained by sonication of the preheated dispersion (Dr. Hielscher sonicator UP400s at 50% amplitude and cycle 1). The vesicle dispersions were then filtered to free them from debris of the sonicator probe. The obtained solutions had a slight bluish tinge indicating small colloidal particles. According to cryo-TEM micrographs, the vesicle diameter was about 40 nm.[32] For this given diameter and a headgroup size of 0.6 nm,[2 33] the number of vesicles per unit volume, N_{ves}, is approximately $1 \times 10^{-6} N_A$ L^{-1}, N_A being Avogadro's number.

Large unilamellar vesicles were prepared by extrusion of the preheated coarse DODAB dispersion through three stacked 200 nm polycarbonate filters (Millipore, hydrophilized PC filters) at 60 °C in three passes (7 bar argon pressure). A highly turbid dispersion resulted from this procedure. The diameter here was determined by cryo-TEM to approximately 160 nm.[11] The number concentration of vesicles, N_{ves}, is then estimated to be $4 \times 10^{-8} N_A$ L^{-1}.

Preparation of the Samples. Typically 100 mL of a 10^{-2} mol/L DODAB vesicle solution was pipetted into a glass vial equipped with a magnetic stirrer. In a second vial, the photoinitiator (DMPA) was dissolved in styrene at concentrations of 0.1 mol/L or lower. The solutions were flushed with argon for 15 min to reduce oxygen. Under stirring, a desired amount of the initiator/monomer solution was injected through a septum into the light protected vial of the vesicle solution (typically 0.21 g, resulting in 2×10^{-2} mol/L overall monomer concentration and 2.3×10^{-4} mol/L overall initiator concentration). The whole dispersion was stirred at room temperature for 2 days to attain equilibrium.[34] The initiator DMPA is only

slightly water-soluble (1×10^{-4} mol/L) but solubilizes preferentially in the amphiphilic aggregate. A partition coefficient $K_p = 2.3 \times 10^4$ was measured by Candau et al.[35] for the partitioning of DMPA between water and hexadecyldimethyl(phenylethyl)ammonium chloride micelles. This surfactant is chemically similar to DODAB and is therefore expected to exhibit a comparable solubilization behavior for DMPA. Probably, the K_p is even higher for DODAB owing to the double-tailed structure. On the basis of this K_p value one can calculate that more than 98% of the photoinitiator would partition into the vesicular phase.

Pulsed-Laser Polymerizations. Photopolymerizations were carried out in a 2 mL thermostated quartz cell (optical path length ~20 mm) in which the monomer-containing vesicle dispersion was injected and placed 10 cm from the laser. When experiments were performed at higher temperatures, the solutions were preheated not longer than 20 min to attain the temperature-dependent monomer equilibrium. The reaction mixture was then injected into the polymerization cell. The cell temperature could be controlled to ±0.1 °C and was monitored by a small resistance element inside the cell.

The irradiation source was a pulsed excimer laser (Lambda Physics LPX110iMC) generating the light at 351 nm (XeF line) and operating at 50 mJ per pulse which corresponds to 1.5×10^{-7} mol of photons per pulse. The pulse width was ca. 20 ns. Repetition rates varied between 1 and 10 Hz and polymerization times were between 1 and 120 min. Conversion had to be higher than ~5% (i.e., 0.2 mg of polymer) to yield sufficient polymer for SEC analysis. Directly after the laser irradiation, 100 μL of the dispersion was withdrawn and diluted in 1.9 mL of methanol (Biosolve, HPLC grade). The residual monomer concentration and consequently conversion was determined by HPLC. The remainder of the sample solution (ca. 1.9 mL) was quenched by cooling and by the addition of a small amount of hydroquinone solution. These samples were subsequently either freeze-dried or dried in a desiccator.

Size Exclusion Chromatography. Prior to SEC analysis, the polymer had to be freed from surfactant. Therefore, the vesicle−polymer hybrid dispersion was first dried and the obtained white powder was then dissolved in ~3 mL of hot THF. After the solution was cooled in a refrigerator, the amphiphile precipitated in large crystals, leaving the polymer solution on top. The top phase was decanted and passed first over a cotton-wool pipet filter and second over a 0.2 μm PTFE syringe-filter (Alltech) to remove residual surfactant crystals and other large contaminants. The obtained polymer solution was then adjusted to a concentration of ~1 mg/mL for SEC analysis. The SEC analyses were carried out using four PLgel (Mixed-C) columns (Polymer Laboratories) at 40 °C. The injection volume was 100 μL and THF was used as eluent at a flow rate of 1 mL/min. A Waters 410 differential refractometer and a Waters 486 UV-detector (operated at a wavelength of 254 nm) were applied for detection. Narrow-distribution polystyrene standards (Polymer Laboratories) with molecular weights ranging from 580 to 7.1×10^6 were used to calibrate the SEC setup.

HPLC Analysis. HPLC analysis was carried out using a Waters HPLC equipment and a Zorbax C-18 reversed phase column. The use of a UV photodiode array detector (Waters 990) permitted calibration at several wavelengths (for styrene 210 and 244 nm). Eluent was a methanol/water mixture 80/20 with a flow of 1 mL/min. The injection volume was 5 μL.

UV Measurements. UV spectra were measured at room temperature with a HP UV−vis diode array spectrophotometer (HP 8451 A) using a quartz cuvette of 1 cm optical path length.

General Considerations for a PLP Experiment: Homogeneous Systems vs Heterogeneous Systems. The kinetics of a PLP experiment in heterogeneous systems deviates in several respects from the behavior in homogeneous systems. The differences between these two cases will be contrasted below.

Homogeneous Systems. In fact, only four parameters are variable when performing PLP experiments: the pulse energy, the initiator concentration, the repetition frequency, $1/t_0$, and the monomer concentration. The first two parameters determine the increase in radical concentration after a pulse, $[\Delta R]$. For *homogeneous* systems, a maximum pseudo-steady-state radical concentration, $[R]_{max}$, will be attained after several pulses, described by[16]

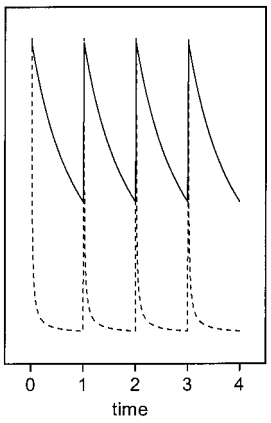

Figure 3. Schematic representation of the radical-time profiles for PLP experiments in bulk systems (solid line) and compartmentalized zero-one systems (dashed line).

$$[R]_{max} = [\Delta R]\left(\frac{1}{2} + \sqrt{\frac{1}{4} + \frac{1}{2k_t[\Delta R]t_0}}\right) \quad (3)$$

Directly after a pulse, the radical concentration decays owing to bimolecular termination and hence, the decay profile depends on the maximum radical concentration and the average termination coefficient, k_t, following the equation

$$[R](t) = \left(2k_t t + \frac{1}{[R]_{max}}\right)^{-1} \quad (4)$$

A typical radical−time profile for a homogeneous system is depicted in Figure 3.

Heterogeneous Systems. A distinctly different behavior is expected for PLP experiments in a *heterogeneous* system. Now, the actual pulsed-polymerization experiment takes place in small "*microreactors*", which are separated from each other. In our case, the reaction volume is given by the number of vesicles per unit volume, N_{ves}, and their individual volume, V_{ves}, which comprises in total only 1% v/v of the sample volume.[21] Due to the small reaction volume the *local* radical concentration at the site of reaction, $[R]_{loc}$, will be about hundred times higher than the *overall* radical concentration, $[R]_{ov}$, according to

$$[R]_{loc} = \frac{[R]_{ov}}{V_{ves}\, N_{ves}} \quad (5)$$

If only *one* radical is present in one small unilamellar vesicle, the *local* radical concentration within the vesicle already amounts to 1×10^{-4} mol/L! The extraordinarily high *local* radical concentrations that can arise in the particles will lead to rapid bimolecular termination (cf. eq 4). However, for termination to occur, it is required that at least two radicals per particle are present. It is therefore more meaningful to regard the average number of radicals per particle, $\bar{n}$, instead of thinking of radical concentrations on a local *volume* basis. It holds that

$$\bar{n} = \frac{[R]_{ov}\, N_A}{N_{ves}} = [R]_{loc} N_A V_{ves} \quad (6)$$

To perform a successful PLP experiment in a heterogeneous system, it would be desirable that the increase in radicals per particle per pulse, $\Delta\bar{n}$, should be ideally above one. If several radicals per particle are present, i.e., $\Delta\bar{n} > 1$, they will either undergo instantaneous bimolecular termination after the pulse

(cf. eq 4) as a consequence of the high radical *local* concentration or exit out of the particle. In either case, maximally one radical per particle can survive and the number of radicals per particle will fall below one almost immediately after the pulse (see scheme in Figure 3). Within the terminology of emulsion polymerization one would call this a "zero−one" system.

Conversely, if $\Delta\bar{n}$ is far less than one, it becomes improbable that a growing polymer chain is terminated by the subsequent pulse, and no structured polymer material can be expected under such conditions.

The foregoing discussion illustrates the paramount importance of the radical concentration with respect to the number of particles for a PLP experiment in heterogeneous systems. To choose the appropriate reaction conditions, particularly the initiator concentration and the pulse energy, it is helpful to estimate first the concentration of radicals that are created in one pulse. This value depends on the number of photons which are produced by a laser pulse, I_0, the reaction volume, V, the initiator efficiency in the medium, φ, and the absorbance, A, of the sample. The absorbance itself obeys the law of Lambert−Beer, $A = \epsilon[\mathrm{I}]d$, where [I] is the initiator concentration, ϵ the extinction coefficient of the initiator at the incident wavelength, and d the optical path length of the cell. Quantitatively this comes down to[37]

$$[\Delta\mathrm{R}] = 2\varphi I_0 (1 - 10^{-A})\frac{1}{V} \tag{7}$$

For the system under investigation we consider the following points:

- an incident intensity, I_0, of 10^{-7} mol of photons that reach the polymerization cell (wavelength 351 nm, 50 mJ, 70% of the beam hits the sample);
- an initiator efficiency, φ, of DMPA of 0.02;[38]
- a reaction volume, V, of 2 mL;
- an overall initiator concentration, [I] of 2.3×10^{-4} mol/L (i.e. 0.1 mol/L based on monomer);
- a molar extinction coefficient of DMPA of $\epsilon_{351} = 255$ L/mol·cm as determined by UV measurements;
- a path length of 2 cm.

In a first approach, we calculate the increase in the *overall* radical concentration after the pulse, $[\Delta\mathrm{R}]_{ov}$, to 2×10^{-7} mol/L, corresponding to $\Delta\bar{n} = 0.2$. Later, the problem of the appropriate initiator concentration will be addressed experimentally.

We must note that the above applied initiator efficiency of $\varphi = 0.02$ is low compared to bulk systems. This value is justified based on the strong effect of the initiator efficiency on the local diffusivity of the radicals in the reaction medium. In the present system, most of the initiator will initially reside in the bilayer. Typical values for the *lateral diffusion of solutes* in bilayers[39] between 10^{-9} cm^2/s and 10^{-7} cm^2/s give an indication of the micro-viscosity in this medium. Such low diffusion coefficients, e.g., 10^{-8} cm^2/s, result in an initiator efficiency of only 0.02.[38]

Note further that we did not take into account a possible attenuation of the incident beam by light scattering. This effect is not easily quantified as to which extent the elastically scattered photons are effectively *lost* for initiator cleavage. Nonetheless, we have to keep in mind that scattering will inevitably lead to inhomogeneity in the illumination of the sample which is an intrinsic problem of photopolymerizations in colloidal samples. To minimize the effect of scattering, we used the smaller, less scattering vesicles (SUVs) for most of the experiments. After optimization of the reaction conditions, we also investigated the larger, highly scattering extruded vesicles. Those results are discussed in the last paragraph of the Results and Discussion.

Results and Discussion

The Minimum Initiator Concentration. To perform a successful PLP experiment in heterogeneous systems, the number of radicals created per pulse should compare fairly well to the number of particles in the sample, in this case vesicles, to guarantee termination in the individual particles by subsequent pulses. That is the essence of the experiment, and it has been pointed out that the initiator concentration plays a key role in this.

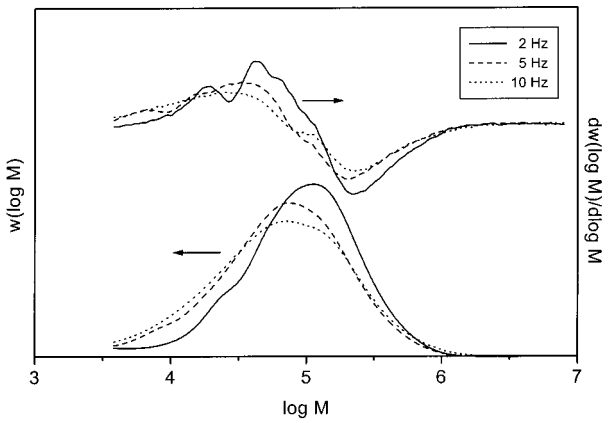

Figure 4. MWDs and derivatives for PLP experiments with SUVs at 20 °C using the minimum initiator concentration of 1.15×10^{-4} mol/L.

On one hand, an initiator concentration of 2.3×10^{-4} mol/L or lower would maximally afford an average increase in number of radicals per particle of $\Delta\bar{n} = 0.2$; i.e., ideal PLP conditions would not be met according to our estimates. On the other hand, one has to realize that an initiator concentration of 2.3×10^{-4} mol/L together with a monomer concentration of 2×10^{-2} mol/L implies that already more than 1% of the solubilized molecules are initiator molecules. Since it was desirable to keep the photoinitiator concentration as low as possible to avoid any unknown effect of the initiator on the structure of the bilayer, we strove for the lowest initiator concentration. To compensate for this, a relatively high pulse energy of 50 mJ was chosen. The minimum threshold concentration of initiator was determined in a series of experiments with increasing overall initiator concentration of 2.3×10^{-5}, 5.8×10^{-5}, and 1.15×10^{-4} mol/L amounting to an estimated increase in radicals per particle after a pulse, $\Delta\bar{n}$, of 0.025, 0.05, and 0.10, respectively. Repetition frequencies of 1, 2, 5, and 10 Hz were used. It turned out that an overall concentration of 1.15×10^{-4} mol/L DMPA was the minimum concentration necessary to find structured MWD revealing pulsed initiated material with the typical overtones (see Figure 4). The experiment suggests that for initiator concentrations greater than 1.15×10^{-4} mol/L, the number of radicals produced at each pulse is large enough to terminate growing polymer chains, and the experiment starts to work in the proper sense of a PLP experiment. According to our earlier estimates, the increase in radical concentration per pulse per vesicle was only $\Delta\bar{n} = 0.1$. Anyhow, this estimate suffers from some uncertainties and obviously, we underestimated the value of $\Delta\bar{n}$ most likely by an overestimate of the number of particles. Pulse repetition rates of 2 and 5 Hz gave the best results. Because of the yet unsatisfying structure of the MWDs, it was decided to increase the initiator concentrations for further experiments to 2.3×10^{-4} mol/L.

The Effect of Pulse Frequency. The dependence of the MWD on the pulse frequency is a typical feature of a PLP experiment and can serve therefore as a quality check for a successful experiment. With higher frequen-

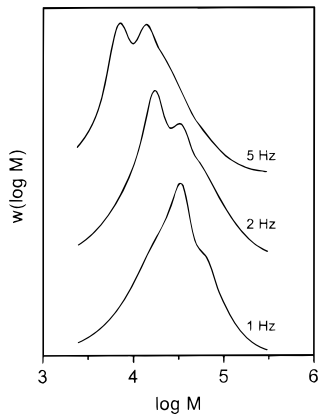

Figure 5. MWDs as a function of frequency for PLP experiments with SUVs at 21 °C using 1.7×10^{-4} mol/L initiator concentration and an overall monomer concentration of 1.5×10^{-2} mol/L at ~15% conversion.

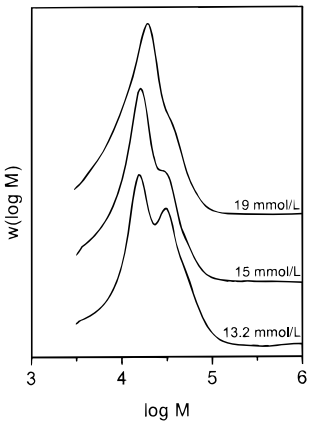

Figure 6. MWDs as a function of overall monomer concentration for PLP experiments with SUVs at 21 °C using a pulse frequency of 2 Hz. Polymerization was stopped at low degrees of conversion (~5%).

cies, the MWD has to shift to lower molecular weights (cf. eq 1). To investigate the effect of the pulse frequency we carried out a set of PLP experiments with SUVs at 21 °C using an overall monomer concentration of 1.5×10^{-2} mol/L (see Figure 5) and analyzing the low conversions (<15%).

The molecular weight distributions are indeed influenced by the pulse frequency in the desired way and hence, the IUPAC requirements for each PLP experiment are fulfilled. We calculate a monomer concentration at the reaction site of 3.48 ± 0.12 mol/L independent of the pulse frequency. Without going into detail about the actual value of the monomer concentration, which we will discuss later on, it is sufficient to notice here that the outcome of the PLP experiment is unperturbed by a change in the pulse frequency—at least within the applied frequency interval.

A closer look at the MWDs reveals that both peak *position* and *shape* of the MWD depend on the frequency. The so-called second overtone of the PLP-originating peak, i.e., the polymer peak in the MWD, which corresponds to a growth time of $2t_0$, is discernible for all frequencies. At higher frequencies, the second overtone becomes more pronounced than for the lower frequencies where the overtone is only indicated by a shoulder on the high molecular weight side of the main peak (see Figure 5, 1 Hz). For shorter dark times, the fraction of radicals that survive until a successive pulse arrives is apparently elevated. We thus deal with radical loss processes that occur during the dark time in the compartmentalized polymerization loci. A shorter dark time clearly allows less radical loss, but what could be the origin of these loss processes? Bimolecular termination within one particle cannot be responsible as a consequence of the compartmentalization and the "zero—one" situation (vide supra). Instead, transfer to monomer, followed by particle exit and termination in the water phase or termination after entry into another particle could be processes that account for a decrease of radicals during the dark time. Our results suggest that these phase transfer events could contribute to the PLP kinetics in the present system.

The Local Monomer Concentration as a Function of the Overall Monomer Concentration. Now that we had found a working experimental recipe and ensured that the pulsed-laser polymerization is performed in a reliable way, we approached our main goal, namely the characterization of the polymer locus by determining the *local* monomer concentration.

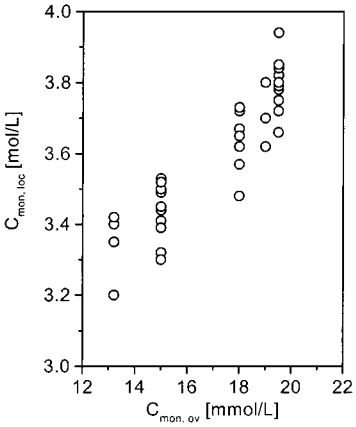

Figure 7. Local monomer concentrations as a function of the overall monomer concentration at 20.5 ± 0.5 °C calculated from PLP experiments with variable pulse frequencies.

We further investigated the concentration at the *site of reaction* as a function of the *overall* monomer concentration. Therefore, a series of PLP experiments with increasing overall monomer concentration was performed at 20 °C using pulse frequencies of 2, 5, and 10 Hz at low degrees of conversion. Figure 6 displays the MWDs for 2 Hz.

Polymeric material was obtained only at global concentrations higher than $\approx 1.3 \times 10^{-2}$ mol/L. In an interval of 1.3×10^{-2} to 2.0×10^{-2} mol/L, the apparent *local* monomer concentration varied between 3.3 and 3.8 mol/L (see Figure 7 and Table 1).

This result is striking in two respects. First, these values are unexpectedly high compared to an estimated monomer concentration in the vesicle *bilayer* of maximally 2.1 mol/L in the case of an overall monomer concentration of 2×10^{-2} mol/L.[40] Second, only a *slight* increase in *local* concentration is noticed with higher *global* concentrations. The *local* concentration in the bilayer increases to a relatively smaller extent (11%) than the *global* concentration (46%). Both observations suggest that the bilayer and the locus of polymerization are *not* identical. What could then be the nature of the polymerization locus? For an explanation it is helpful to recall the morphological picture (cf. Figure 2). Online SANS measurements proved that a small polymer bead evolves within the beginning stages of the poly-

Table 1. Averaged Calculated Local Monomer Concentrations, $[M]_{loc}$, as a Function of Temperature, *T*, Overall Monomer Concentration, $[M]_{ov}$, and Vesicle Type

vesicle type	*T* (°C)	$[M]_{ov}$ (mol/L)	$[M]_{loc}$ (mol/L)	σ_n (mol/L)[a]
SUV	20.5	1.32×10^{-2}	3.34	0.09
SUV	20.5	1.50×10^{-2}	3.48	0.12
SUV	21.0	1.81×10^{-2}	3.61	0.09
SUV	20.0	1.90×10^{-2}	3.73	0.08
SUV	21.0	1.95×10^{-2}	3.79	0.06
SUV	30.0	1.90×10^{-2}	3.31	0.14
SUV	40.0	1.90×10^{-2}	3.16	0.09
SUV	50.0	1.90×10^{-2}	2.93	0.15
SUV	60.0	1.90×10^{-2}	2.58	0.17
LUV	25.0	1.99×10^{-2}	4.54	0.18
LUV	60.0	1.99×10^{-2}	3.29	0.05

[a] σ_n represents the standard deviation of the local monomer concentrations.

merization process.[14] Such a polymer bead could be easily swollen with monomer supplied by the attached vesicle. It is established that the saturation swelling of a polymer sphere rests on its radius,[15,23,27,41−44] especially for radii below 30 nm being relevant here. To quote some model data:[15] for styrene at 50 °C a saturation swelling concentration of 3.3 mol/L is calculated for a radius of 10 nm, which would be comparable to the present situation.

Therefore, we strongly believe that the polymerization in vesicles proceeds within a polymer locus that has been identified as a polymer bead by morphological measurements. This polymerization locus quickly attracts the monomer being solubilized in the vesicle and any growing radicals. The monomer partitioning between polymer bead and parental vesicle at lower *overall* concentrations seems relatively more in favor of the locus of polymerization, at the expense of the bilayer. This accounts for the comparatively small effect of the overall monomer concentration on the local concentration.

From a mechanistic point of view, it is interesting as well to compare the shape of the MWDs with increasing monomer concentrations (see Figure 6). It is noticed that overtones and high molecular material are more pronounced at lower monomer concentrations. A simple explanation is given by the fact that a lower monomer concentration implicitly means a lower *initiator* concentration as we kept the ratio monomer/initiator constant for reasons of comparison. A lower level of initiator produces a lower radical flux per pulse and leads to the occurrence of high molecular material (vide supra).

The Effect of Temperature. The previous results suggested that the polymerization locus is a polymer bead which is supplied by monomer from the attached vesicle. We have seen that the determination of the *local* monomer concentration then gives insight in the partitioning between locus of polymerization and monomer reservoir. It is generally expected that the temperature influences significantly the partition behavior between polymer phase, vesicle phase and aqueous phase. To study the effect of temperature a series of experiments with 2.0×10^{-2} mol/L styrene concentration was carried out at 20, 30, 40, 50, and 60 °C using pulse frequencies of 2 and 5 Hz. Pulsing times were adapted to keep conversion below 15%. The calculated monomer concentrations are summarized in Table 1 and they are plotted in Figure 8 as a function of temperature. Remarkably, the apparent concentration decreases from 3.8 mol/L at 20 °C to 2.6 mol/L at 60 °C. This drop in

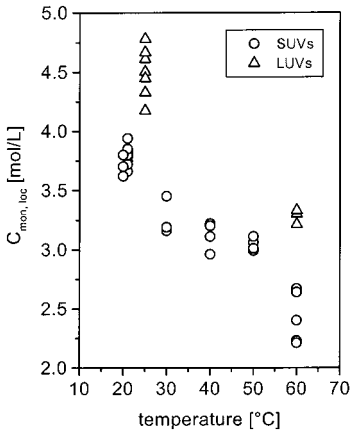

Figure 8. Local monomer concentrations as a function of temperature for SUVs and LUVs calculated from PLP experiments with 2.3×10^{-4} mol/L initiator concentration, variable pulse frequencies and an overall monomer concentration of $(1.9 \pm 0.1) \times 10^{-2}$ mol/L.

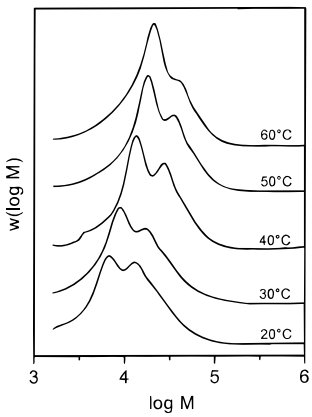

Figure 9. MWDs as a function of temperature for PLP experiments with SUVs using 2.3×10^{-4} mol/L initiator concentration, 5 Hz pulse frequency and an overall monomer concentration of 1.9×10^{-2} mol/L at conversions <15%.

accessible monomer concentration in the polymerization locus is ascribed to a changed partitioning in favor of the bilayer. At elevated temperatures, the solubilization capacity of the bilayer rises[45] and less monomer is consequently released to the polymerization locus. Additionally, the water solubility of styrene is enhanced at higher temperatures and diminishes the total monomer concentration in the heterogeneous phase.

Again, a closer inspection of the corresponding MWDs (Figure 9) reveals mechanistic information. The overtone becomes gradually less prominent at higher temperatures indicating that radical loss processes are intensified at elevated temperatures. An increasing importance of chain transfer relative to propagation could lead to a loss of growing radicals during the dark time and could thus readily account for the observed effect.

The Monomer Concentration as a Function of Conversion. All previous data corroborate the hypothesis that the polymer bead is the locus of polymerization rather than the bilayer. Next, we investigated the local monomer concentration as a function of *conversion* to decide whether the nature of the polymerization locus changes with conversion. Two series PLP experiments, denoted SUVs(1) and -(2), with SUVs were performed using an initiator concentration of 2.3×10^{-4} mol/L, a pulse frequency of 2 Hz, and an overall monomer

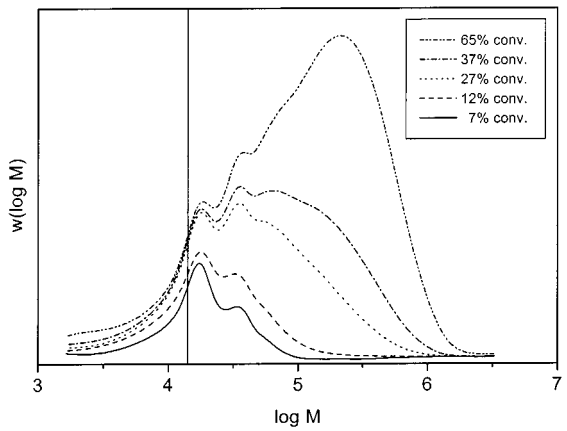

Figure 10. MWDs as a function of conversion for PLP experiments with SUVs at 21 °C using 2 Hz pulse frequency and 2.3×10^{-4} mol/L initiator concentration.

concentration of 1.95×10^{-2} mol/L. Figure 10 shows a set of conversion-normalized cumulative MWDs with increasing conversion for the series SUVs(1).

At low conversions (<30%), the MWDs exhibit the typical shape of PLP material. Within this interval, the inflection point at the low molecular weight side of the PLP peak does not shift with conversion. On average we find a value of 3.79 ± 0.06 mol/L which is in line with earlier measured values (see Table 1). It is remarkable that the calculated monomer concentration does not decrease with increasing conversion.

At higher conversions (>30%), the MWDs show some peculiar characteristics:

- High molecular weight material becomes pronounced.
- The amount of PLP material hardly increases.
- The second overtone remains present throughout the whole range of conversion.

Taking these observations into consideration, it appears that the experiment stops working in the sense of a pulsed polymerization experiment above ∼30% conversion. Featureless material then starts to be formed at the high molecular weight side of the MWD. The initially produced PLP material contributes to the MWD and is still recognized by the overtone characteristics. This effect can be ascribed to a drop in radical flux per pulse caused by a drop in initiator concentration. When a conversion of about 30% is reached, a considerable amount of initiator will be consumed. The number of radicals created per pulse then falls below a certain threshold value where not enough radicals are created to terminate most of the growing chains; i.e., we suspect $\Delta\bar{n}$ to be far below 1. Since bimolecular termination after a pulse is no longer the main chain-stopping event, transfer to monomer becomes a more important process. In other words, the experiment shifts from a *PLP-dominated* regime to a *transfer-dominated* regime. To check for the contribution of transfer to the MWD we plotted the logarithm of the number distribution, $n(M)$, against the molecular weight and determine the apparent chain transfer constant.[46−48] It yields

$$\lim_{M\to\infty}\left(\frac{\ln n(M)}{M}\right) = -\frac{1}{M_0}\frac{k_{tr}[M] + k_t[R]}{k_p[M]} \equiv -\frac{\Lambda}{M_0} \quad (8)$$

where k_{tr} represents the transfer rate coefficient for transfer to monomer and M_0 is the molecular weight of the monomer unit. The value of Λ can be obtained from

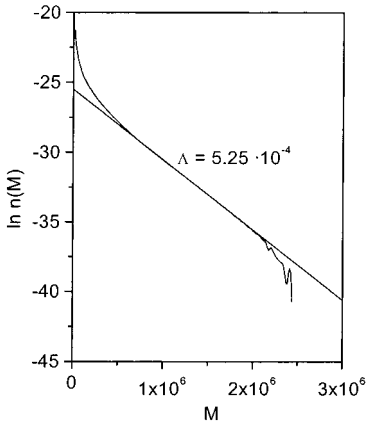

Figure 11. Logarithm of the number distribution plotted against the molecular weight in order to determine Λ. Here it was plotted for the MWD of the PLP experiments with SUVs at 21 °C and 65% conversion.

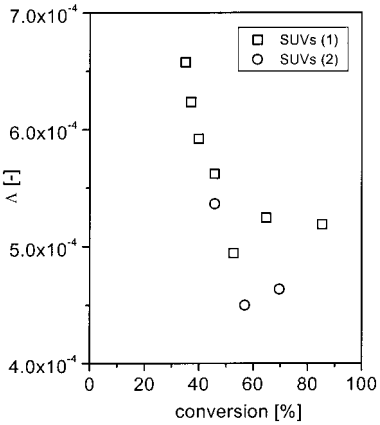

Figure 12. Plot of Λ derived from cumulative MWDs of PLP experiments with SUVs at 21 °C using 2 Hz pulse frequency and 2.3×10^{-4} mol/L initiator concentration as a function of conversion.

the MWD through the relationship

$$\Lambda = -M_0(\text{slope of the linear region of } \ln n(M)) \quad (9)$$

A typical plot is shown in Figure 11 and the derived values for Λ are plotted in Figure 12 vs conversion. As expected, the values decay with increasing conversion as result of the smaller contribution of bimolecular termination. They seem to level off at an average value of $\Lambda \approx 5 \times 10^{-4}$. In the limiting case of no contribution of bimolecular termination to the MWD, Λ would correspond to the chain transfer constant, C_{tr}. The found value compares favorably to literature values for styrene of 5×10^{-4} (50 °C, low initiator concentrations).[47]

Summarizing, it can be said that the MWD as a function of conversion changes from an interval that is PLP-dominated (up to ∼30−40% conversion) to an interval that is transfer-dominated. The appearance of marked overtones without the prominent presence of high molecular weight tailing indicates that the experiment is conducted under conditions where the number of created radicals and the number of particles at least match within the PLP-dominated interval.

One method to circumvent the problem of initiator depletion with increasing conversion would be the application of an electron beam which delivers a constant number of radicals independent of conversion.[29,49] However, own explorative experiments using an electron

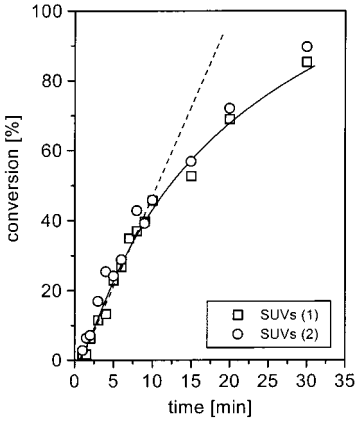

Figure 13. Combined conversion−time plots for PLP experiments with SUVs at 21 °C using 2 Hz pulse frequency and 2.3×10^{-4} mol/L initiator concentration. The solid line is a guide to the eye. The dashed line is a linear fit to the data up to 10 min polymerization time.

beam as irradiation source[50] for the vesicle system induced colloidal instability of the dispersion, probably due to electrostatic effects,[51] and was therefore discarded.

Finally note that the decreasing *overall* monomer concentration with conversion should clearly shift the MWD to *low* molecular weights within the PLP-dominated interval. However, it is highly interesting—with respect to the mechanism of polymerization in vesicles—to observe that the apparent monomer concentration at the *locus* of polymerization stays constant *at least* in the first interval (up to 40% conversion). This accounts for the nature of the locus: Seemingly, the locus is supplied with a constant monomer feed from the vesicle reservoir.

Conversion−Time Behavior. The analysis of the conversion data provides a deeper insight into the kinetics of polymerization in vesicles. Two series of experiments, denoted SUVs(1) and -(2), were performed to construct conversion plots using identical reaction conditions as in the previous experiment. The reproducibility was well within experimental error (see Figure 13).

The rate of polymerization remained constant for the first 10 min of the reaction, corresponding to about 40% conversion, before it decreased nonlinearly with time. The initially constant rate implies that both $\bar{n}_{ave}$ and monomer concentration are also constant, which is kinetically analogous to an interval II emulsion polymerization.[15] The decrease in rate after this period would then be analogous to interval III where the monomer concentration drops as a consequence of monomer depletion. However, the deceleration could also be explained by a decrease in radical flux due to initiator consumption.

In this light, the MWD data and the conversion data are favorably in line and the conversion data corroborates the assumption of a constant local monomer concentration up to about 40% conversion. Kinetically, the reaction can be described by an interval II emulsion polymerization[15]

$$\frac{dx}{dt} = \frac{k_p[M]_{loc}\,[R]_{ave,ov}}{[M]_{ov}} = \frac{k_p[M]_{loc}\,N_{ves}\,\bar{n}_{ave}}{[M]_{ov}\,N_A} \quad (10)$$

where x represents the fractional conversion, $[M]_{loc}$ the local monomer concentration at the site of reaction, $[M]_{ov}$ the overall monomer concentration, and $\bar{n}_{ave}$ the time-averaged, average number of radicals per particle (cf. eq 6).

Except for $\bar{n}_{ave}$ and $[M]_{loc}$, all parameters in above equation are known. The latter, $[M]_{loc}$, has been readily determined by the PLP analysis to be 3.8 mol/L. We then calculate the radical concentrations (see Table 2).

The resulting average number of radicals per particle, $\bar{n}_{ave}$, of ~0.06 appears very low and cannot be reconciled with the idea of a successful PLP experiment. Most likely, we overestimated the number of vesicles leading to a considerable underestimation of $\bar{n}_{ave}$. Our earlier observations when searching for the minimum initiator concentrations led us to the same conclusion.

The Effect of Vesicle Size. In a last set of experiments we studied the effect of vesicle size by employing large unilamellar vesicles LUVs. It has been pointed out that the vesicle size determines the polymer bead size of the parachute structure. Therefore, the vesicle size is expected to play a role in the polymerization kinetics. Pulsed-laser polymerizations were performed with styrene (1.99×10^{-2} mol/L) at 25 and 60 °C and laser frequencies of 2 and 5 Hz as a function of conversion. Figure 14 shows the results for a pulse frequency of 5 Hz.

The build-up of transfer dominated material is, in analogy to SUVs, noticed at higher conversions. Derived apparent transfer constants (on average $C_{tr} = 4.3 \times 10^{-4}$ at 25 °C) equally correspond to earlier found values for the SUV experiments.

The fact that the monomer concentrations for LUVs (4.5 mol/L at 25 °C, 3.3 mol/L at 60 °C, see Figure 8) exceed those calculated for SUVs is considered as an interesting result. Obviously the size of the polymer locus relates to its monomer concentration. This is not surprising within the framework of the above presented mechanistic model: After formation of polymer locus, the polymer swells with monomer provided by the bilayer. A competitive partitioning of the solubilized monomer between the vesicle bilayer and the polymer particle results. Dependent on the bead size, i.e., dependent on the vesicle size, the polymer could swell to a lower or higher degree. Model calculations[15] on the saturation swelling of a polystyrene bead of 25 nm radius with styrene indicate values of about 4.7 mol/L. This value compares fairly to our findings.

Finally, the conversion analysis resembles the data for the SUVs except for the fact that conversion scales up to 60% linear with time (see Figure 15). The rate of polymerization is significantly lower than for SUVs although the local monomer concentration in LUVs surpasses the concentration measured for SUVs (see Table 2). As a consequence of the strong turbidity of the sample the radical production seems considerably reduced. Therefore, the initiator lasts up to higher conversions and provides a constant rate. We can only speculate that the monomer concentration remains constant in this interval, too. The MWDs do not allow to retrieve unambiguous data on the monomer concentration within the transfer-dominated interval, i.e., above 40% conversion. Again, the number of radicals per particle can be calculated from the rate data. The average number of radicals per particle amounts here $\bar{n}_{ave} = 0.224$, which seems a more realistic estimate.

Conclusions

On the basis of data on the monomer concentration at the locus of polymerization combined with rate data,

Table 2. Parameters for Conversion-Dependent PLP Experiments at 2 Hz Using an Initiator Concentration of 2.3 × 10^{-4} mol/L

vesicle type	T (°C)	k_p (L/mol·s)	$[M]_{ov}$ (mol/L)	dx/dt (s^{-1})	$[M]_{loc}$ (mol/L)	$[R]_{ave,ov}$ (mol/L)	$\bar{n}_{ave}$
SUVs(1)	21	71.9	1.95×10^{-2}	8.5×10^{-4}	3.79	6.1×10^{-8}	0.061
SUVs(2)	21	71.9	1.81×10^{-2}	7.9×10^{-4}	3.61	5.5×10^{-8}	0.055
LUVs	25	85.9	1.99×10^{-2}	1.8×19^{-4}	4.54	8.9×10^{-9}	0.224

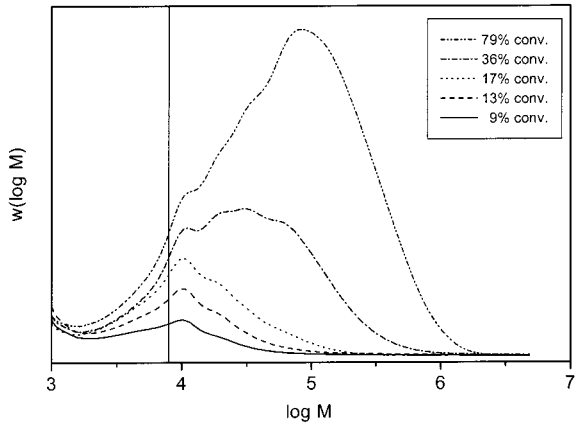

Figure 14. MWDs as a function of conversion for PLP experiments with LUVs at 25 °C using 5 Hz pulse frequency and 2.3 × 10^{-4} mol/L initiator concentration.

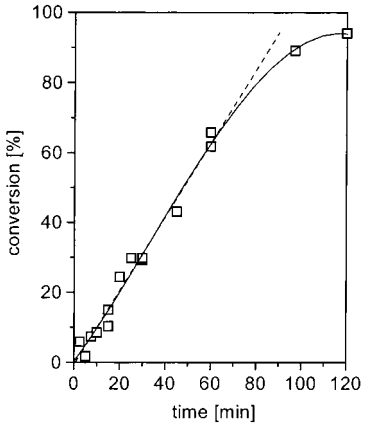

Figure 15. Conversion−time plot for PLP experiments with LUVs at 25 °C using 2 Hz pulse frequency and 2.3 × 10^{-4} mol/L initiator concentration. The solid line is a guide to the eye. The dashed line is a linear fit to the data points up to 60 min polymerization time.

we postulate that the locus of polymerization is the phase-separated polymer bead formed at the beginning of the polymerization. The initially created polymer nucleus swells with monomer supplied by the attached vesicle reservoir. Polymerization further proceeds within this polymer particle where constant monomer concentrations are provided up to at least 40% conversion.

This working hypothesis can account for all our observations. In essence, the observed phenomena were independent of total monomer concentration, temperature and vesicle size. The variation of these reaction conditions, however, offered a more detailed knowledge on the partitioning of monomer between the three involved phases: vesicle bilayer, polymerization site, and water.

It was recognized that the heterogeneous nature of the system significantly complicates the experimental performance for PLP studies. Ideal conditions have to be chosen and optimized such that the number of radicals per vesicles is just high enough to allow bimolecular termination after successive pulses. The local initiator concentration and the partitioning of initiator then become relevant problems. Our PLP experiments as a function of conversion showed that the depletion of initiator can cause the experiment to shift from an initially PLP-dominated domain to a transfer-dominated domain. In fact, the experimental window for successful PLP experiments in this system is rather small.

The application of the PLP technique to heterogeneous systems can be particularly advantageous as it provides simultaneously *thermodynamic* information on the locus of polymerization next to *kinetic* data. Despite experimental problems that are to be overcome, we feel that the PLP technique can be a unique tool to explore microphase separated colloidal particles, like the vesicle−polymer hybrids, with respect to the spatial distribution of monomers and thus can function as a "kinetic microscope".

Acknowledgment. This work was financially supported by The Netherlands Organization for Scientific Research (NWO/CW). We gratefully acknowledge Wieb Kingma for the careful SEC analyses of countless samples. We thank John de Kock and Bart Manders for stimulating and helpful discussions.

References and Notes

(1) *Polymerisation in Organized Media*; Paleos, C. M., Ed.; Gordon and Breach Science Publishers: Philadelphia, PA, 1992.
(2) Antonietti, M.; Göltner, C. *Angew. Chem., Int. Ed.* **1997**, *36*, 991−928 and references therein.
(3) Meier, W. *Current Opin. Colloid Interface Sci.* **1999**, *4*, 6−14 and references therein.
(4) *Emulsion Polymerization and Emulsion Polymers*; Lovell, P. A., El-Aasser, M. S., Eds.; Wiley: Chichester, England, 1997.
(5) Murtagh, J.; Thomas, J. K. *Faraday Discuss. Chem. Soc.* **1986**, *81*, 127−136.
(6) Kurja, J.; Nolte, R. J. M.; Maxwell, I. A.; German, A. L. *Polymer* **1993**, *34*, 2045−2049.
(7) Poulain, N.; Nakache, E.; Pina, A.; Levesque, G. J. *Polym. Sci., Polym. Chem.* **1996**, *34*, 729−737.
(8) Morgan, J. D.; Johnson, C. A.; Kaler, E. W. *Langmuir* **1997**, *13*, 6447−6451.
(9) Hotz, J.; Meier, W. *Langmuir* **1998**, *14*, 1031−1036.
(10) Hotz, J.; Meier, W. *Adv. Mater.* **1998**, *10*, 1387−1390.
(11) Jung, M.; Hubert, D. H. W.; Bomans, P. H. H.; Frederik, P. M.; Meuldijk, J.; van Herk, A. M.; Fischer, H.; German, A. L. *Langmuir* **1997**, *13*, 6877−6880.
(12) Jung, M.; Hubert, D. H. W.; van Veldhoven, E.; Frederik, P. M.; Blandamer, M. J.; Briggs, B.; Visser, A. J. W. G.; van Herk, A. M.; German, A. L. *Langmuir* **1999**, in press.
(13) Jung, M.; Hubert, D. H. W.; van Veldhoven, E.; Frederik, P. M.; van Herk, A. M.; German, A. L. Submitted to *Langmuir*.
(14) Jung, M.; Robinson, B. H.; Steytler, D. C.; Heenan, R. K.; German, A. L. Submitted to *Langmuir*.
(15) Gilbert, R. G. *Emulsion Polymerisation: A Mechanistic Approach*; Academic Press: London, 1995.
(16) Olaj, O. F.; Bitai, I.; Hinkelmann, F. *Makromol. Chem.* **1987**, *188*, 1689−1702.
(17) Buback, M.; Gilbert, R. G.; Hutchinson, R. A.; Klumperman, B.; Kuchta, F. D.; Manders, B. G.; O'Driscoll, K. F.; Russell, G. T.; Schweer, J. *Macromol. Chem. Phys.* **1995**, *196*, 3267−3280.
(18) Gilbert, R. G. *Pure Appl. Chem.* **1992**, *64*, 1563−1567.
(19) Gilbert, R. G. *Pure Appl. Chem.* **1996**, *68*, 1491−1494.

(20) Beuermann, S.; Buback, M.; Davis, T. P.; Gilbert, R. G.; Hutchinson, R. A.; Olaj, O. F.; Russell, G. T.; Schweer, J.; van Herk, A. M. *Macromol. Chem. Phys.* **1997**, *198*, 1545−1560.
(21) Beuermann, S.; Buback, M. In *Controlled Radical Polymerization*; Matyjazsewski, K., Ed.; ACS Symposium Series 685; American Chemical Society: Washington, DC, 1998; Chapter 6.
(22) van Herk, A. M. *J. Macromol. Sci.—Rev. Macromol. Chem. Phys.* **1997**, C*37* (4), 633−648.
(23) Manders, L. G. Pulsed Initiation Polymerization. Ph.D. Thesis, Eindhoven University of Technology, 1997.
(24) Holdcroft, S.; Guillet, J. E. *J. Polym. Sci., Part A: Polym. Chem.* **1990**, *28*, 1823−1829.
(25) Manders, B. G.; van Herk, A. M.; German, A. L.; Sarnecki, J.; Schomacker, R.; Schweer, J. *Makromol. Chem., Rapid Commun.* **1993**, *14*, 693−701.
(26) Manders, B. G.; van Herk, A. M.; German, A. L. *Macromol. Theory. Simul.* **1995**, *4*, 325−333.
(27) Schweer, J.; van Herk, A. M.; Pijpers, R. J.; Manders, B. G.; German, A. L. *Macromol. Symp.* **1995**, *92*, 31−41.
(28) Bayer, A. G. Ger. Offen. DE 44 13 003 A1, 19 October 1995; *Chem. Abstr.* **199X**, *124*, 88571.
(29) van Herk, A. M.; de Brouwer, H.; Manders, B. G.; Luthjens, L. H.; Hom, M. L.; Hummel, A. *Macromolecules* **1996**, *29*, 1027−1030.
(30) Botman, J. I. M.; Derksen, A. T. A. M.; van Herk, A. M.; Jung, M.; Kuchta, F.-D.; Manders, L. G.; Timmmermans, C. J.; de Voigt, M. J. A. *Nucl. Instr. Methods B* **1998**, *139*, 490−494.
(31) For review on vesicle preparation techniques, see: Lasic, D. D. *Liposomes: From Physics to Applications*; Elsevier: Amsterdam, 1993; Chapter 3.
(32) Size derived from cryo-TEM micrographs; see: Zirkzee, H. F. A Novel Approach to the Encapsulation of Silica Particles. Ph.D. Thesis, Eindhoven University of Technology, 1997.
(33) Shapovalov, V.; Tronin, A. *Langmuir* **1997**, *13*, 4870−4876.
(34) Hubert, D. H. W. Surfactant Vesicles in Templating Approaches. Ph.D. Thesis, Eindhoven University of Technology, 1999; p 74.
(35) Cochin, D.; Zana, R.; Candau, F. *Macromolecules* **1993**, *26*, 5765−5771.
(36) The molar volume of DODAB is given with 0.705 L/mol, i.e. for a 1×10^{-2} mol/L DODAB dispersion 7 mL/L. Taking into account the volume of solubilized styrene, i.e., 2.3 mL/L, one calculates roughly a total of 1% v/v heterophase volume. See for molar volume: Aramaki, K.; Kuneida, H. *Colloid Polym. Sci.* **1999**, *277*, 34−40.
(37) Odian, G. *Principles of Polymerization*; John Wiley & Sons: New York, 1991; p 226.
(38) Kurdikar, D. L.; Peppas, N. A. *Macromolecules* **1994**, *27*, 733−739.
(39) Almeida, P. F. F.; Vaz, W. L. C. In *Structure and Dynamics of Membranes*; Sackmann, E., Lipowsky, R., Eds.; Elsevier/North-Holland: Amsterdam, 1995; Chapter 6.
(40) On the basis of partitioning data (see ref 12), one calculates that about 88% of the monomer is solubilized in the vesicle bilayer. In the case of 2×10^{-2} mol/L overall monomer concentration, 1.76×10^{-2} mol/L styrene are solubilized in 7 mL/L pseudo-phase volume (see ref 36). This results in a monomer concentration in the bilayer of 2.1 mol/L, provided that the *full* bilayer volume is accessible for solubilization.
(41) Morton, M.; Kaizermann, S.; Altier, W. *J. Colloid Sci.* **1954**, *9*, 300−312.
(42) Vanzo, E.; Marchessault, R. H.; Stannet, V. *J. Colloid Sci.* **1965**, *20*, 62−71.
(43) Gardon, J. L. *J. Polym. Sci. A-1* **1968**, *6*, 2859−2879.
(44) Tseng, C. M.; El-Aasser, M. S.; Vanderhoff, J. W. In *Computer Applications in Applied Polymer Sciences*; Rovder, E., Ed.; ACS Symposium Series 197; American Chemical Society: Washington, DC, 1982; p 197.
(45) Hubert, D. H. W. Surfactant Vesicles in Templating Approaches. Ph.D. Thesis, Eindhoven University of Technology, 1999; p 65.
(46) Clay, P. A.; Gilbert, R. G. *Macromolecules* **1995**, *28*, 552−569.
(47) Clay, P. A.; Gilbert, R. G.; Russell, G. T. *Macromolecules* **1997**, *30*, 1935−1946.
(48) Moad, G.; Moad, C. *Macromolecules* **1996**, *29*, 7727−7733.
(49) *Radiation Chemistry: Principles and Applications*; Farhataziz, Rodgers, M. A. J., Eds.; VCH Publishers: New York, 1987.
(50) For experimental details concerning the electron beam facility see reference [30].
(51) Thomas, J. K. In *Radiation Chemistry: Principles and Applications*; Farhataziz, Rodgers, M. A. J., Eds.; VCH Publishers: New York, 1987; Chapter 12.

MA9919211